JOURNAL OF CATALYSIS 38, 19–32 (1975)

Interaction Between the Active Components and Support in the Co–Mo–Al_2O_3 System

II. The Role of Sodium and Cobalt

P. RATNASAMY, A. V. RAMASWAMY, K. BANERJEE, D. K. SHARMA AND N. RAY

Indian Institute of Petroleum, Dehradun (U.P.), India

Received June 13, 1974; revised December 3, 1974

The kinetics of reduction of MoO_3, molybdenum–alumina, cobalt–alumina and cobalt–molybdenum–alumina in H_2 has been investigated. The equation of Avrami and Erofeev assuming the formation and growth of nuclei describes mathematically most appropriately the rate of reduction for all these samples. The presence of sodium in the alumina support profoundly affects the reducibility curves. In its absence, cobalt has an inhibitory influence on the reduction of molybdenum–alumina. However, in the presence of sodium, cobalt accelerates the reduction process. The extent of reduction of all these samples is limited by the water evolved during the process. For 14 different cobalt–molybdenum–alumina catalysts, as their reducibility increases, the catalytic activity passes through a maximum and falls at higher values of reducibility.

It is postulated that in the presence of sodium, most of the cobalt occurs in the form of Co_3O_4 which on reduction forms the metal. Once formed, cobalt metal accelerates the reduction of supported MoO_3. In the absence of sodium, cobalt, now occurring mostly as well-dispersed Co^{2+} ions which are not reduced during the reduction, strongly retains the water evolved during the process and thereby suppresses the reduction of MoO_3. A model of the catalyst surface and the probable role of cobalt and sodium in the catalyst formulation are advanced to account for the observed dependence of hydrodesulfurization activity on the reducibility of the samples.

INTRODUCTION

Even though a considerable amount of work has been reported on the nature of the cobalt and molybdenum species in hydrodesulfurization catalysts (*1–5*), the influence of the structural features of the support on the formation of such species and their relevance for the catalytic activity of the Co–Mo–Al_2O_3 system as a whole has not been adequately investigated. In an earlier paper (*6*), we had reported that cobalt, present in the subsurface layers of alumina, prevents the sintering and phase transformations of the support which process would have otherwise been facilitated by molybdenum oxide, especially during the calcination of the oxide prior to sulfidation. In the present study, we have used the reducibility (in hydrogen), acidity and ir spectroscopic techniques to characterize the oxide surface. A correlation between reducibility and steady state catalytic activity for kerosene hydrodesulfurization has been observed. It is found that sodium ions in the support influence the nature of the active cobalt species formed on the oxide precursor and thereby influence the reducibility and catalytic activity of the sample. A probable additional role of cobalt in the catalyst formulation is advanced based on the results.

EXPERIMENTAL METHODS

The samples were prepared as indicated in Table 1. The isothermal reduction runs

TABLE 1
DESCRIPTION OF THE SAMPLES USED IN THE REDUCTION STUDIES

Sample	Preparation	Activated at (°C)	Surface area (m^2/g)	% Al_2O_3:Co_3O_4:MoO_3:Na
Al	Obtained from boehmite	550	240	100:0:0:0
AlNa	Obtained from Al by impregnation with Na	550	240	99.98:0:0:0.02
MoO_3	Decomposition of ammonium paramolybdate (AP)	550	1.7	0:0:100:0
Co_3O_4	Decomposition of cobalt carbonate at 500°C	500		0:100:0:0
MoAl	Impregnation of Al with AP	550	230	87.5:0:12.5:0
MoAlNa	Impregnation of AlNa with AP	550	230	87.48:0:12.5:0.02
CoAl	Impregnation of Al with cobalt nitrate (CN)	550	240	97.5:2.5:0:0
CoAl900	Calcination of CoAl at 900°C for 24 hr	550	25	97.5:2.5:0:0
CoAlNa	Impregnation of AlNa with CN	550	240	97.48:2.5:0:0.02
CoMoAl(S)	Simultaneous impregnation of Al with AP and CN	550	240	85:2.5:12.5:0
CoMoAlNa(S)	Simultaneous impregnation of AlNa with AP and CN	550	240	84.98:2.5:12.5:0.02
CoMoAlNa	AP impregnated "on top" of CoAlNa	550	240	84.98:2.5:12.5:0.02
MoCoAlNa	CN impregnated "on top" of MoAlNa	550	240	84.98:2.5:12.5:0.02

were carried out in a TG apparatus (Fischer; 1 mg/mV full scale deflection). A Linseis model DTA equipment was used to follow the heat changes during the reduction. The typical procedure for a kinetic run was as follows: After the sample (size 88–125 nm; 40 mg in all cases except otherwise noted) was loaded in the TG bucket, the apparatus was flushed with dry He–N_2 mixture (150 ml(STP)/min) and the sample was heated to and maintained at 110°C until no further weight loss was observed. The sample was then heated to the reduction temperature (490–550°C) and held constant at that temperature until no further change in weight was observed during at least 1 hr. The He–N_2 mixture was then switched off and H_2 was let in (150 ml(STP)/min). Changes in the weight of the sample were also noted simultaneously. Only weight changes observed after the fifth minute were used in the calculations. The acidity measurements were made using *n*-butylamine and H_0 indicators (*7*). To estimate the sulfur reversibly bound on the surface of MoAlNa and CoMoAlNa, the samples were sulfided in a glass reactor at 250°C and at 1 atm pressure using a H_2–CS_2 mixture ($H_2/CS_2 = 10$) for 5 hr. The reversibly bound sulfur was then estimated by first flushing the reactor with He–N_2 for 10 min at 250°C and then passing H_2 for 1 hr and absorbing the evolved H_2S in a NaOH solution (1 *M*). The sulfur in the solution was estimated by conventional wet techniques. The ir spectra of the samples (in the form of thin discs) were measured using a Beckman ir 12 spectrometer. The setting of the instrument was: slit, 1 × stand. slit; gain, 5.0%; period, 2 sec; scanning speed, 8 cm^{-1}; spectral slit width, 0.6 mm at 800 cm^{-1} and spectral resolution, of the order of 2 cm^{-1}.

The hydrodesulfurization experiments were carried out in a steel reactor (catalyst vol, 5 cc; 16–20 mesh). The kerosene feed had the following characteristics: boiling range, 149–291°C; sulfur, 0.6% by wt; and smoke point, 21 mm. The catalysts were

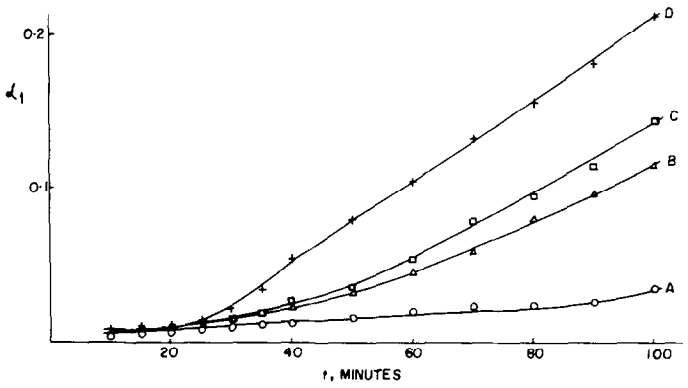

FIG. 1. Reduction of MoO_3 at 490, 510, 530, and 550°C (A, B, C, and D, respectively).

first sulfided at 230–280°C for 6 hr using the feed along with H_2 (LHSV = 6; 20 kg/cm^2; gas/oil = 1000). The catalysts were then stabilized at the reaction conditions (LHSV = 6; 320°C; 20 kg/cm^2; gas/oil = 1000) for about 15 hr before their desulfurization activity (expressed as percentage removal of sulfur) was determined.

RESULTS

Reduction studies. Preliminary experiments had indicated that below 450°C, the water formed in the reduction readsorbed on the sample leading to a lack of reproducibility in the kinetic data. Similar difficulties have also been reported by Lipsch (*8*). The reduction experiments reported here were hence conducted in the range 490–550°C. Figure 1 shows the effect of temperature on the fraction reduced for MoO_3. Here $\alpha_1 = (W_i - W_t)/\Delta W$ where W_i is the initial weight, W_t the weight at time t and ΔW is the calculated weight loss for the process, $MoO_3 + H_2 \rightarrow MoO_2 + H_2O$.

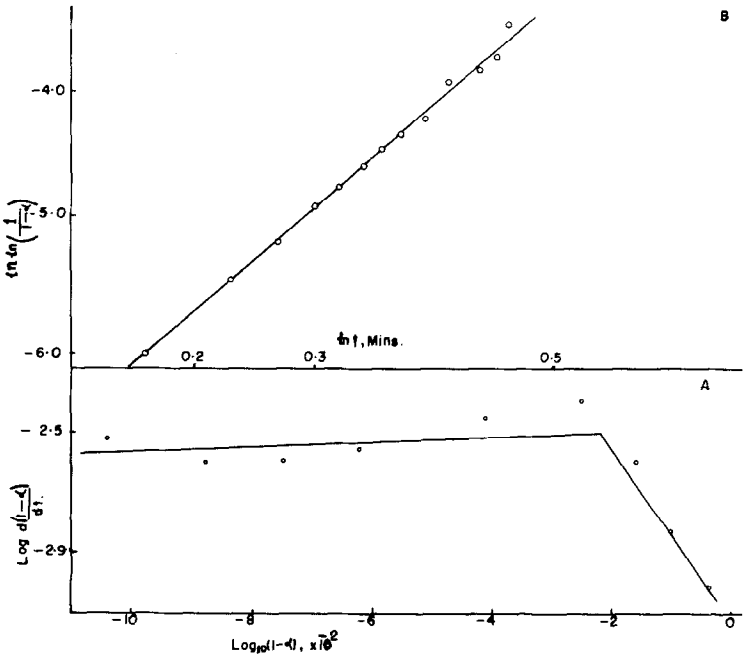

FIG. 2A. Van't Hoff plot for the reduction of MoO_3 at 490°C; (B) nuclei-growth plot for the reduction of MoO_3 at 490°C; comparison of calculated values (straight line, $m = 0.86$) with experimental data (points).

Each set of data (α vs t) were analyzed in the following manner: first, a Van't Hoff differential analysis (*9*) was performed by plotting log $(-d(1-\alpha)/dt)$ vs log $(1-\alpha)$ to check whether the concept of a reaction order is applicable at all to that particular system. Figure 2A shows the Van't Hoff plot for MoO_3 at 490°C. The fact that a straight line is not obtained means that rate equations based on the concept of an order of reaction are mathematically inappropriate for expressing and correlating the data. Next, the data were fitted, by the least squares technique, successively, to the equations and reaction models indicated in Table 2. Table 3 compares the validity of the different models. It is seen that the nuclei-growth model of Avrami–Erofeev fit the data best under the conditions studied. This is also confirmed by Fig. 2B which presents a nuclei-growth analysis plot. The fit between the calculated and experimental values is quite satisfactory. It might be noted here that the Avrami–Erofeev model assumes that when a solid is converted to a second phase, the chemical reaction is initiated at certain discrete points called nucleus-forming sites. The period during which this occurs is called the induction or nucleation period. This leads to the formation of submicroscopic particles of the product-solid phase called nuclei. As the reaction proceeds further the nuclei grow in size. This period is called the accelerating stage. In the third stage, further growth of the nuclei leads to their overlap resulting in a reduction in the area of the reaction-interface and a consequent deceleration of the reaction which continues until the reactant is consumed. A sigmoid-shaped curve is usually observed in the kinetics of such processes.

The reducibility of MoAl and MoAlNa are shown in Fig. 3A. Blank experiments carried out with Al and AlNa indicated a negligible weight loss on changing the carrier gas from $He-N_2$ to H_2 at the reduction temperature. The observed small differences, however, have been taken into consideration while calculating the α_1 values. The sigmoid shape of the $\alpha_1 - t$ curves, faintly noted in Fig. 1 is quite evident in Fig. 3A. It is to be emphasized that even though the initial rate of reduction of MoAl and MoAlNa is higher than that of MoO_3, the final level of reduction (α^{max}, not shown in Figs. 1 and 3A) was much higher for MoO_3. (The further reduction of MoAl and MoAlNa came to an end after about 2 hr whereas the reduction of MoO_3

TABLE 2
MODELS AND CORRESPONDING EQUATIONS FOR THE REDUCTION PROCESS

Rate controlling mechanism	Model	Equation	Ref.[a]
I. Diffusion of reactant through a continuous product layer	Jander	$(1-(1-\alpha)^{1/3})^2 = k_1 t$	(*1*)
	Kroger–Ziegler	$(1-(1-\alpha)^{1/3})^2 = k_2 \ln t$	(*2*)
	Dunwald–Wagner	$\ln 6/2\ (1-\alpha) = k_3 t$	(*3*)
	Ginstling–Brounshtein	$1 - 3(1-\alpha)^{2/3} + 2(1-\alpha) = k_4 t$	(*4*)
II. Nuclei-formation and growth	Avrami and Erofeev	$\ln 1/1 - \alpha = (k_5 t)^m$	(*5*)
III. Reaction at phase boundary	Contracting sphere	$1 - (1-\alpha)^{1/3} = k_6 t$	(*6*)

[a] References:

1. Jander, W., *Z. Anorg. Allg. Chem.* **163,** 1 (1927).
2. Kroger, C., and Ziegler, G., *Glastech. Ber.* **26,** 346 (1953).
3. Dunwald, H., and Wagner, C., *Z. Phys. Chem., Abt. B* **24,** 53 (1934).
4. Ginstling, A.M., and Brounshtein, B.I., *J. Appl. Chem. USSR* **23,** 1327 (1950).
5. a. Avrami, M., *J. Chem. Phys.* **9,** 177 (1941).
b. Erofeev, B.V., *C.R. Acad. Sci. USSR* **52,** 511 (1946).
6. Garn, P.D., CRC Critical *Rev. Anal. Chem.* 65 (1972).

TABLE 3
EVALUATION OF THE DIFFERENT MODELS FOR THE REDUCTION PROCESS[a]

Model		Samples						
		MoO_3	MoAl	CoMoAl(S)	MoAlNa	CoMoAlNa(S)	CoAl	COAlNa
		Rate constants (min^{-1}, 10^{-3})						
Jander	k_1	0.0009 (10)	0.5000 (6)	0.0678 (7)	0.6763 (8)	2.7392 (9)	1.4584 (6)	2.8744 (13)
Kroger–Ziegler	k_2	10.0112 (20)	6.4470 (16)	0.8472 (14)	9.5131 (10)	33.7801 (15)	19.6200 (15)	34.7410 (25)
Dunwald–Wagner	k_3	−0.4030	7.9531 (5)	2.4210 (6)	9.9391 (8)	25.1123 (6)	15.8501 (4)	24.4501 (8)
Ginstling–Brounshtein	k_4	0.0020 (12)	1.2890 (6)	0.1888 (5)	1.7202 (6)	5.8640 (8)	3.3827 (4)	5.5612 (9)
Avrami–Erofeev	m	0.86 ± 0.01	1.23 ± 0.04	0.70 ± 0.02	0.82 ± 0.07	1.26 ± 0.10	0.69 ± 0.02	1.29 ± 0.03
	k_5	0.1791 (2)	9.886 (3)	1.7020 (3)	11.1920 (4)	26.1812 (6)	17.6216 (3)	20.7567 (2)
Contracting sphere	k_6	0.1087 (4)	2.601 (4)	1.0422 (5)	3.1556 (7)	6.6681 (7)	4.567 (5)	6.00 (2)

[a] All the reductions were carried out at 490°C and a H_2 flow of 150 ml (STP)/min. The values in parentheses refer to the percentage relative standard deviation by regression.

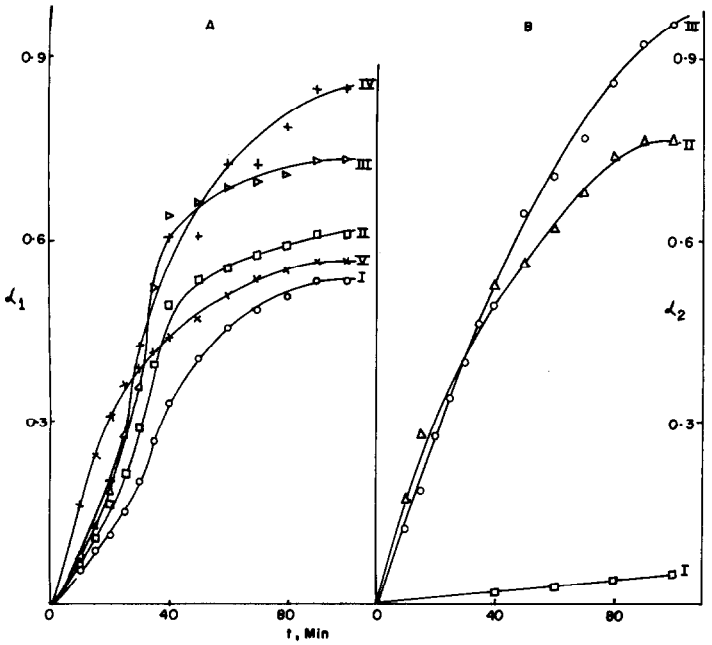

FIG. 3A. Reduction of MoAl at 490, 510, 530, and 550°C (I, II, III, and IV, respectively) and MoAlNa at 490°C (V); (B) reduction of CoAl900, CoAl, and CoAlNa at 490°C (I, II, and III, respectively).

continued even after 5 hr.) Two features may thus be noted: (1) alumina inhibits the final reduction level of supported MoO_3, in accordance with the results of Sondag *et al.* (*10*). (2) The initial rates of reduction of MoAl and MoAlNa, however, are higher than that of MoO_3 by at least an order of magnitude. The origin of this effect is discussed below. Figure 3B depicts the reduction kinetics of CoAl, CoAlNa and CoAl900. Here, α_2 is defined similar to α_1; ΔW now corresponds to the weight loss during the reaction, $Co_3O_4 + 4\ H_2 \rightarrow 3\ Co + 4\ H_2O$. The bright blue color as well as X-ray measurements (NBS circular No. 9,539, 1959) had indicated that CoAl900 contains most of the cobalt as cobalt-aluminate. Its negligible reducibility (Fig. 3B) is in accord with Richardson's results (*11*). Under the same conditions of reduction, Co_3O_4 underwent complete reduction to the metallic state in about 10 min. The higher reducibility of CoAlNa compared to CoAl, thus indicates that in the absence of sodium, cobalt probably enters the Al^{3+} vacancies of the support in which position it is unlikely to get reduced to the metallic state in H_2. When present, sodium occupies these positions preferentially and hence most of the cobalt is converted into Co_3O_4 (or some other easily reducible oxide) which forms the metal on reduction, thus accounting for the observed differences between CoAl and CoAlNa (Fig. 3B). Keeling had observed (*12*) a similar phenomenon in the cobalt–nickel–alumina system. It should be added here that both CoAl and CoAlNa were obtained by impregnation of cobalt nitrate on *calcined* alumina. Ashley and Mitchell who prepared a similar sample but using a *hydrous* alumina found (*4*) no evidence for the presence of Co_3O_4. Tomlinson *et al.* (*13*), on the other hand, adopting a preparative procedure similar to ours, interpreted their magnetic susceptibility data on the basis of a two phase model: a β phase consisting of Co_3O_4 and a δ phase made up of well-dispersed Co^{2+} ions on the alumina support. It is only the former which will be reduced

in H_2. It is clear that the relative proportions of these two phases depend critically on the preparative procedure adopted.

Figure 4A shows the influence of sodium on the reducibility of cobalt–molybdenum–alumina. Here, in the calculation of α_3, ΔW is the weight loss corresponding to the process, $Co_3O_4 \cdot MoO_3 + 5\ H_2 \rightarrow 3\ Co + MoO_2 + 5\ H_2O$. The much larger reducibility of CoMoAlNa(S) compared to CoMoAl(S) further supports the postulate that in the presence of sodium Co_3O_4 is formed which is reduced to the metal in H_2. The presence of metallic cobalt accelerates the reduction of the MoO_3 phase. An additional interesting feature, however, emerges on comparing the reducibility curves at 490°C of MoAl with CoMoAl(S) and MoAlNa with CoMoAlNa(S), respectively. While cobalt inhibits the reduction of MoO_3 in the absence of sodium, it has an enhancing effect when sodium is present (i.e., $\alpha_{CoMoAl(S)} < \alpha_{MoAl}$ but $\alpha_{CoMoAlNa(S)} > \alpha_{MoAlNa}$). While the enhancement of the reduction of MoO_3 by metallic cobalt has been well described in the literature (*14*), its inhibiting effect has not so far been reported. This inhibition is probably due to the fact that in the absence of sodium the precursors that lead to cobalt metal (Co_3O_4, for example) are not present on the catalyst surface. The higher reducibility of MoCoAlNa compared to CoMoAlNa (Fig. 4B) is also due to a similar reason. The formation of Co_3O_4 is more likely when cobalt is impregnated "on top" of molybdena than directly on the alumina surface. In the latter case, more cobalt ions are expected to interact directly with the alumina surface and hence resist reduction in hydrogen.

The influence of sample weight on the reducibility of MoO_3, MoAl, and CoMoAl is shown in Fig. 5. The fact that the rate is inversely dependent on sample mass indicates that the reverse reaction (i.e., reaction of water with MoO_2) limits the overall kinetics for all these samples. The inhibitory effect of water evolved during the reaction on the further reduction of pure MoO_3 has also been reported by Vasilev *et al.* (*15*). The retarding influence of the support on the reduction of MoO_3 is probably due to the stronger retention of the evolved water by the strong acid sites of

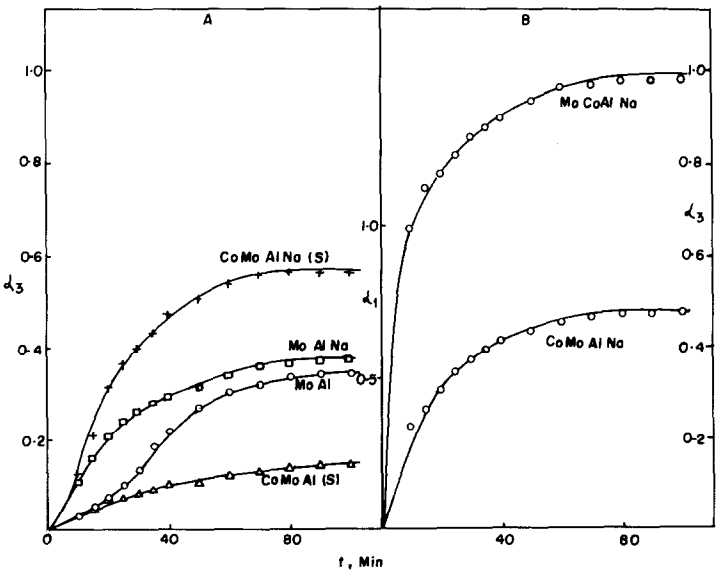

FIG. 4. Influence of sodium. (A) Reduction of CoMoAl(S), MoAl, MoAlNa and CoMoAlNa(S), respectively, at 490°C; (B) reduction of CoMoAlNa and MoCoAlNa, respectively.

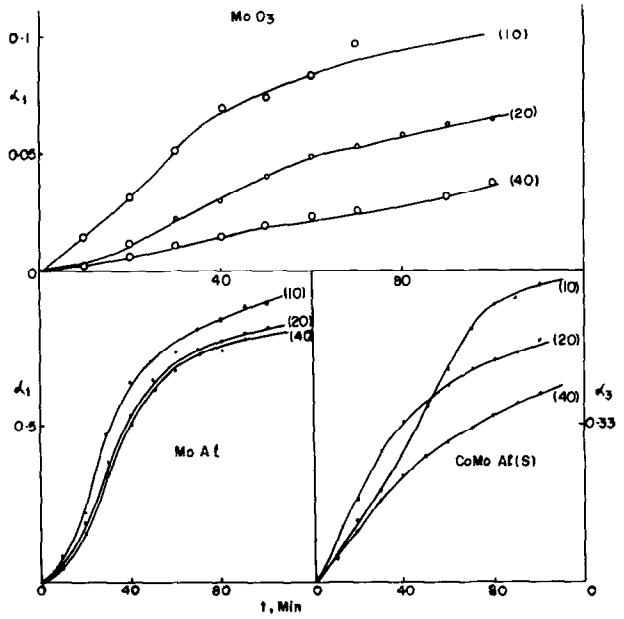

FIG. 5. Influence of sample weight on the kinetics of reduction of MoO_3, MoAl, and CoMoAl(S), respectively.

the adjoining support regions thus facilitating the occurrence of the reverse reaction. The acidity values given in Table 4 also support the above picture. In the absence of sodium, CoMoAl(S) is more acidic than MoAl. When sodium is present, however they have similar acidic properties. In other words, the interaction between the cobalt and molybdenum moeties to generate strong acid sites is inhibited by the Na^+ concentration of the alumina support. The stronger acid sites in CoMoAl(S) retain the water evolved during reduction more strongly thereby inhibiting the reduction process. The absence of such sites in CoMoAlNa(S) removes this inhibitory influence of cobalt (*27*). Table 3 gives a summary of the rate constants obtained by the nuclei-growth model for the various samples. It is to be noted that this model gave the best mathematical fit to the kinetic data for all the samples studied. For MoO_3, MoAl, and CoMoAl(S) reduction runs were carried out at 490, 510, 530 and 550°C. The rate constants obtained were fitted to the Arrhenius equation. Apparent activation energies of 137.3, 18.3 and 50.6 kcal/mole were calculated for MoO_3, MoAl, and CoMoAl(S), respectively, confirming that mass transport in the gaseous phase is not

TABLE 4
SURFACE ACID STRENGTH DISTRIBUTION IN THE Co–Mo–Al_2O_3 SYSTEM

Sample	pK_a value of the indicators				
	+5.0	+3.3	+2.0	−3.0	−5.6
	n-Butylamine titer[a]				
Al	4.2	3.4	3.4	3.4	0.0
AlNa	0.9	0.9	0.9	0.9	0.0
MoAlNa	11.1	9.6	9.6	9.6	6.0
CoAlNa	7.0	6.2	6.2	6.2	0.0
CoMoAlNa	12.8	11.8	11.8	10.6	7.0
MoCoAlNa	9.6	8.9	8.9	8.9	5.0
CoMoAlNa(S)	11.1	8.9	8.9	8.9	6.5
MoAl	13.4	10.0	10.0	10.0	5.0
CoMoAl(S)	17.0	16.0	16.0	11.0	9.4
CoAl	6.7	6.6	6.6	6.6	0.0
MoO_3	124.5	106.4	106.4	84.3	64.2

[a] Number of *n*-butylamine molecules consumed by 1000 Å^2 of the surface of the samples; the values are reproducible to about ±0.8.

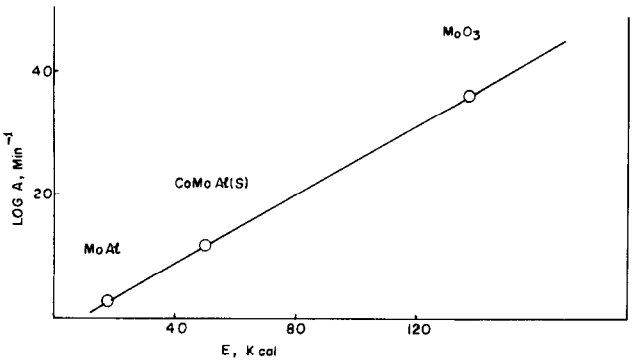

FIG. 6. The "compensation effect" in the reduction of MoO_3, MoAl, and CoMoAl(S), respectively.

a limiting factor under our experimental conditions. An interesting feature of the results is the existence of the "compensation effect" in this system as shown in Fig. 6. An increase in E with the number of active sites has been observed in other systems also (*16*). Sosnovsky (*17*) attributed it to mutual interaction among the active sites when their density is high. When there is a strong interaction between the active sites, the energy of each site will be lowered, resulting in an increased value of E associated with the increase in A. In our case, the active sites on MoAl and CoMoAl(S) are most probably those oxygen atoms which differ from those in MoO_3 mainly in regard to the extent of separation from each other. That is, the basic MoO_3 structure is more or less preserved on going from MoO_3 to MoAl, and CoMoAl(S); the units are, however, dispersed to a larger extent. This conclusion is in agreement with those of Lipsch and Schuit (*18*). It is to be stated, however, that this applies only to the reducible part. The nonreducible molybdenum species on the support may have a different configuration (see discussion below).

Infrared spectroscopy. The influence of reduction (for 30 min in hydrogen at 490°C) on the ir spectra of MoO_3, MoAl, and CoMoAl(S) is shown in Fig. 7. The

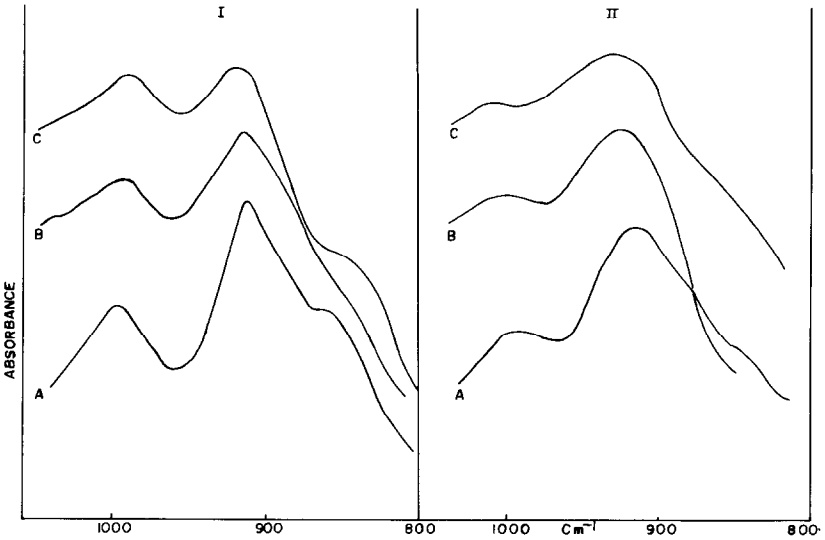

FIG. 7. (I) Infrared spectra of MoO_3, MoAl, and CoMoAl(S) (A, B, and C, respectively); (II) ir spectra after reduction in H_2 of the same samples.

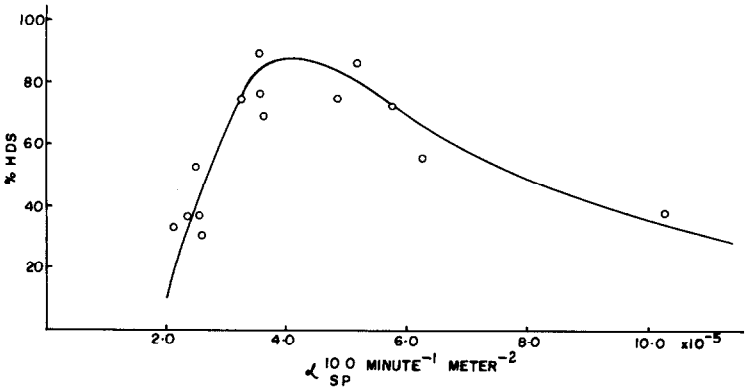

FIG. 8. Correlation between the catalytic activity and specific reducibility of different cobalt–molybdenum–alumina catalysts.

"terminal" metal–oxygen bond responsible for the 990–1000 cm^{-1} band (*19*) is seen to be the first species to lose oxygen in the presence of hydrogen.

Sulfidation and catalytic studies. Under the conditions of sulfidation employed, the amount of sulfur reversibly bound by MoAlNa and CoMoAlNa(S) are 0.70 and 0.93% by wt, respectively. Under identical conditions, CoAlNa contained negligible amounts of reversibly bound sulfur though the total sulfur uptake was still appreciable. The hydrodesulfurization activity of 14 catalysts (commercial as well as our own, all containing Co, Mo, and Na) of approximately the same composition is plotted against their specific reducibility, α_{sp}^{100} [α_3^{100} per unit time per unit surface area (BET)] of the catalyst. The value of 100 in α_{sp}^{100} refers to the value of α_3 at the 100th minute. For all the catalysts α_3^{100} did not differ significantly from α_3^{max}) in Fig. 8. The activity of the catalysts seems to pass through a maximum as their reducibility is increased. It may be added here that catalysts containing little or no sodium had a low α_{sp}^{100} as well as a low catalytic activity.

DISCUSSION

Reduction studies. MoO_3 has a ReO_3-type structure with layers of MoO_6 octahedra (Fig. 9). Three of the oxygen atoms of the octahedra are common to three MoO_6 units and two common to two MoO_6 octahedra. The sixth oxygen atom (indicated by black circles in Fig. 9) is unshared and is bound to only one octahedron. Successive layers are packed such that the unshared oxygen atoms of one layer point down between the apices of the neighboring layers. Both ir (Fig. 7) and X-ray (*20*) studies reveal that these sixth oxygen atoms have a higher vibration frequency than the other five [the temperature factor $B = 9.5 \times 10^{-3}$ nm^2 for these oxygens compared to 6.3 and 5.6×10^{-3} nm^2 for the others (*20*)]. A special feature of the ReO_3-type of lattice is the range of stable shear structures that may be formed from it (*21*). The reduction of MoO_3 in hydrogen, for example, might be visualized as follows: Initially a few oxygen vacancies are created by the removal of oxygen atoms by hydrogen. These vacancies then agglomerate into vacancy discs.

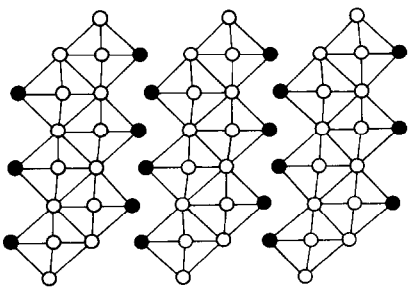

FIG. 9. The structure of MoO_3.

When these discs lie in a shear plane, their collapse along the shear vector leads to an area of the shear plane which is bound by a dislocation loop. Further reduction, then extends the dislocation loop and carries the shear plane through the crystal structure. A given level of reduction, therefore, corresponds to a certain density of shear planes (per unit volume of the crystal). The observed conformity of the reduction kinetics to the nuclei-growth model as well as changes in the ir spectrum of reduced MoO_3 (Fig. 7) are in agreement with the above picture. Formation of the oxygen vacancies corresponds to the nuclei-formation stage; their further growth by diffusion and agglomeration constitutes the nuclei-growth stage.

When MoO_3 is supported on alumina, due to the greater dispersion and interaction with the support, the forces of interaction between the MoO_6 octahedra are reduced. (This is the origin of the "compensation effect", see Fig. 6). Hence, the rates of nuclei formation and initial growth are enhanced (Fig. 3A). However, due to the strong retention of the evolved water molecules by the adjoining alumina surface regions, reduction is arrested earlier and the final level of reduction attained is lower than in pure MoO_3. [It may be recalled (Fig. 5) that over all the samples the rate of reduction was limited by the reverse reaction (*15*)]. Cobalt, when supported on alumina can exist in at least two different structural positions (*12*): as an ion in the Al_2O_3 lattice (for example, Co^{2+} in Al^{3+} vanancies on the alumina surface, the δ phase), or as part of an oxide phase (Co_3O_4, the β phase). In the former position, it is not reduced by hydrogen (*12*). In the latter form, it is easily reducible to the metal. All our supported cobalt–alumina and cobalt–molybdenum–alumina samples contain both the forms, the relative proportions being strongly dependent on the sodium content of the support as well as other preparative procedures. Sodium ions, when present on the support, increase the proportion of the β phase ($\alpha_{CoAlNa} > \alpha_{CoAl}$). Apparently, they occupy the Al^{3+} vacancies thus depriving the Co^{2+} ions of adsorption sites. The influence of cobalt on the reducibility of molybdenum–alumina depends on the relative proportions of δ and β phase cobalt on the alumina surface. The former (found to a larger extent in samples free of sodium) interacting structurally with both the alumina and MoO_3 phases, remains unreduced under the reduction conditions and attenuates the reduction of the dispersed MoO_3 by enhancing the retention of the water formed during reduction ($\alpha_{CoMoAl(S)} > \alpha_{MoAl}$, Fig. 4A). When sodium ions are present, cobalt, now mostly present in the form of Co_3O_4, is converted to the metal under the reduction conditions and accelerates the reduction of the MoO_3 phase.

Correlation between reducibility and catalytic activity. The significant features of our study in this domain may be summarized as follows: (a) The amount of sulfur *reversibly* held on the surface is more on cobalt–molybdenum–alumina than on molybdenum–alumina. (b) A correlation, Fig. 8, exists between the desulfurization activity and the specific reducibility of cobalt–molybdenum–alumina catalysts. For purposes of discussion, we might also include the following points from the literature: (c) The initial hydrodesulfurization activities of both molybdenum–alumina and cobalt–molybdenum–alumina are comparable, the superiority of the latter manifesting itself mainly in the steady state activity (*3*). (d) Molybdenum is associated with the desulfurization reaction while isomerization and hydrogenation are thought to proceed over active centers involving mainly cobalt (*22*). (e) Both cobalt and molybdenum are only partly sulfided during the hydrodesulfurization process (*5,23*) and (f) well-defined compounds of cobalt and molybdenum (like

$CoMoO_4$ or $CoAl_2O_4$, etc.) are absent in the precursor oxide and in the sulfided state (*5*).

Now, Roman and Delmon (*24*) from studies of the promoter and carrier effects in the reduction of NiO/SiO_2, have distinguished three types of nickel oxide that can be formed on silica. A first fraction which is not reducible, a second "initiable" fraction whose reduction can be initiated by promoters like copper and a third fraction which is spontaneously reducible. On the basis of our results we suggest the following similar model for the surface structure of a "typical" cobalt–molybdenum–alumina catalyst (2–5% Co as Co_3O_4, 12–15% Mo as MoO_3 and 100–500 ppm Na): Mo occurs in three different forms on the surface of alumina, phase A, wherein chemical interaction with the support is so intimate that the Mo ions are not reduced in hydrogen even at high temperatures [It is likely that the Mo atoms of this phase under the influence of the support, adopt a tetrahedral coordination. The conflicting values for the proportions of tetrahedral and octahedral molybdenum obtained by Ashley and Mitchell (*4*), on the one hand, and Lipsch and Schuit (*18*), on the other, is probably due to the different concentrations of phase A in their samples], phase B which has minimal interaction with the support and a high reducibility and phase C which is partially reducible in the presence of promoters like cobalt metal. Phase C is most likely a monolayer of molybdenum oxide whose perturbation by the underlying support, while less than that of phase A, is still much higher than that of phase B. In the presence of sodium, a substantial part of cobalt occurs as Co_3O_4 which is converted under the reduction conditions to cobalt metal. In hydrogen, this cobalt metal enhances the reducibility of phase B and renders phase C partially reducible. The complete reduction of both phases B and C to the metal is prevented by dispersed, unreduced Co^{2+} ions which are structurally associated with both phases B and C. The exact nature of this association is not clear. The relative proportions of Co^{2+} and Co^0 control the degree of reduction attained by phase C. The attenuation of the reducibility of MoO_3 by Co^{2+} also explains the general observation that the use of molybdena–alumina catalysts (without cobalt) in hydrodesulfurization processes results in the catalyst becoming excessively reduced (very pyrophoric when exposed to air). Under reduction–sulfidation conditions, the partly sulfided molybdenum ions in phase C will be coordinated to both sulfur and oxygen (it may be mentioned here that Armour *et al.* (*5*) did find evidence for the presence of such thiomolybdate species on their sulfided catalysts from their diffuse reflectance spectra), while those in phase B are expected to be mostly converted to the corresponding sulfides. The molybdenum ions in phase A are unlikely to be affected by the reduction/sulfidation treatments. In the partly sulfided phase C, the sulfur atoms are coordinated with surface anion vacancies associated with molybdenum. These anions vacancies, in turn, have been created by the partial reduction process. In the absence of cobalt and sodium even this partial reduction of phase C would not have occurred to a significant extent. The sulfur atoms associated with phase C are expected to be more loosely bound than those involved in the formation of sulfides of molybdenum in phase B. [H_2S is not evolved on passing H_2 over pure MoS_2 at 250°C (*25, 26*)]. The larger observed value of reversibly bound sulfur on CoMoAlNa(S) compared to MoAlNa supports the above picture. This model also explains the observed correlation between reducibility and hydrodesulfurization activity (Fig. 8); A low value of reducibility indicates that most of the molybdenum ions are in the form of phase A. A very high value, on the contrary, is indicative of the preponderance of phase B. Intermediate values reveal a large fraction of the impregnated molybdenum ions as phase C.

Catalytic activity for the hydrodesulfurization reaction is associated mainly with phase C [and especially with its surface anion vacancies wherein sulfur atoms may be reversibly coordinated (*2*)]. At low values of α_{sp}^{100} the percentage desulfurization is low due to the catalytic inactivity of phase A. The catalytic activity is again low at large α_{sp}^{100} values because most of the molybdenum occurs as the MoS_x, (probably as large crystallites of MoS_2) phase B. It is only in the intermediate phase C region with its large number of sites wherein sulfur may be reversibly bound that maximum catalytic activity is to be expected as indeed observed experimentally. The promoting effect of cobalt thus consists in ensuring a proper balance between the oxygen and sulfur atoms associated with molybdenum in phase C. In addition to this role, part of cobalt in either the metallic and/or sulfided form will hydrogenate the diolefins originating from the desulfurization reaction, preventing the formation and accumulation of "coke" precursors on the catalyst surface and thus maintaining a higher level of activity in the steady state. Molybdenum–alumina lacking this hydrogenation component will gradually deteriorate in activity due to the larger deposition of coke on its surface as observed in practice. Other transition elements like Mn, Zn, and Fe are also known (*3*) to enter lattice positions on the alumina and stabilize it against phase transitions. The uniqueness of cobalt (and probably nickel also) is due to the fact that under the reaction conditions it forms species (like Co^0 and Co^{2+}) which can regulate both the reduction of MoO_3 to the desired extent as well as hydrogenate the diolefins and olefins that result from the desulfurization step.

CONCLUSIONS

In the Co–Mo–Al_2O_3 system not only is there a structural interaction between the cobalt and molybdenum constituents, but the nature of this interaction itself is a function of the structural features of the support (like sodium concentration, surface Al^{3+} vacancies, etc.). Even though the active center for the desulfurization reaction involves only molybdenum, cobalt exerts a promoting effect in the creation of these sites and keeping the surface "clean" by hydrogenating the diolefins and other coke precursors. The concentration and nature of such promoter cobalt species, in turn, depend on the sodium concentration and other surface features of the alumina support. Thus, all the three constituents (Co, Mo, and Al_2O_3) form a true interacting system and it is not possible to discuss the nature of any one of them without reference to the other two.

ACKNOWLEDGMENT

We thank Dr. Shobti and Mr. Nautiyal of I. P. E. for the computer facilities extended to us. We are grateful to Drs. M. G. Krishna and K. K. Bhattacharyya for encouragement and support. We also thank Messrs. G. Balamalliah and R. P. Mehrotra for useful discussions.

REFERENCES

1. Mitchell, P. C. H., "The Chemistry of some Hydrodesulfurisation Catalysts Containing Molybdenum," Climax Molybdenum Co., London, 1967.
2. Lipsch, J. M. J. G., thesis, Eindhoven, 1968.
3. De Beer, V. H. J., Van Sintfiet, T. H. M., Engelen, J. F., Van Haandel, A. C., Wolfs, M. W. J., Amberg, C. H., and Schuit, G. C. A., *J. Catal.* **27,** 357 (1972).
4. Ashley, J. H., and Mitchell, P. C. H., *J. Chem. Soc. A,* 2821 (1968).
5. Armour, A. W., Ashley, J. H., and Mitchell, P. C. H., *Amer. Chem. Soc., Div. Petrol. Chem. Prepr.* **16,** A116 (1971).
6. Ratnasamy, P., Mehrotra, R. P., and Ramaswamy, A. V., *J. Catal.* **32,** 63 (1974).
7. Hirschler, A. E., and Schneider, A., *J. Chem. Eng. Data* **6,** 313 (1961).
8. Ref. (*2*), p. 52.
9. Hulbert, S. F., *in* "Thermal Analysis" (R. F. Schwenker, and P. D. Garn, Eds.), Vol. 2, p. 1013. Academic Press, New York 1969.
10. Sondag, R., Kim, D. Q., and Marion, F., *C. R. Acad. Sci.* **259,** 4704 (1964).
11. Richardson, J. T., *Ind. Eng. Chem. Fundam.* **3,** 154 (1964).

12. Keeling, R. O., Jr., *Develop. Appl. Spectrosc.* **2,** 263 (1962).
13. Tomlinson, J. R., Keeling, R. O., Rymer, G. T., and Bridges, J. M., *Actes Congr. Int. Catal., 2nd, 1960* Pap. No. 90 (1961).
14. Masson, J., Delmon, B., and Nechtschein, J., *C. R. Acad. Sci.* **266,** 428 (1968).
15. Vasilev, K., Nikolov, T., and Chimbinlev, M., *God. Vissh. Khimikotekhnol. Inst.* **14,** 321 (1971); *Chem. Abstr.* **77,** 104213 c (1972).
16. Cremer, E., *in* "Advances in Catalysis" (W. G. Frankenburg, V. I. Komarewsky and E. K. Rideal, Eds.), Vol. 7, p. 75. Academic Press, New York, (1955).
17. Sosnovsky, H. M. C., *J. Phys. Chem. Solids.* **10,** 304 (1959).
18. Lipsch, J. M. J. G., and Schuit, G. C. A., *J. Catal.* **15,** 174 (1969).
19. Barraclough, C. G., Lewis, J., and Nyholm, R. S., *J. Chem. Soc.* 3552 (1959).
20. Kihlborg, L., *Ark. Kemi.* **21,** 357 (1963).
21. Krebs, H., "Fundamentals of Inorganic Chemistry," p. 314. McGraw-Hill, London, 1968, (Engl. Transl.).
22. Desikan, P., and Amberg, C. H., *Can. J. Chem.* **42,** 843 (1964).
23. Ahuja, S. P., Derrien, M. L., and Le Page, J. F., *Ind. Eng. Chem. Prod. Res. Dev.* **9,** 272 (1970).
24. Roman, A., and Delmon, B., *J. Catal.* **30,** 333 (1973).
25. Ratnasamy, P., and Leonard, A. J., *J. Catal.* **26,** 352 (1972).
26. Ratnasamy, P., Rodrigue, L., and Leonard, A. J., *J. Phys. Chem.* **77,** 2242 (1973).
27. Ratnasamy P., Sharma L. D., and Sharma D. K., *J. Phys. Chem.* **78,** 2069 (1974).